MOLECULAR AND CELLULAR BIOLOGY, Oct. 2001, p. 7047–7053 Vol. 21, No. 20
0270-7306/01/$04.00+0 DOI: 10.1128/MCB.21.20.7047–7053.2001

Gene Targeting of Envoplakin, a Cytoskeletal Linker Protein and Precursor of the Epidermal Cornified Envelope

ARTO MÄÄTTÄ,† TERESA DiCOLANDREA,‡ KAREN GROOT, AND FIONA M. WATT*

Imperial Cancer Research Fund, London WC2A 3PX, United Kingdom

Received 11 May 2001/Accepted 10 July 2001

Envoplakin, a member of the plakin family of cytoskeletal linker proteins, is localized in desmosomes of stratified epithelial cells and is a component of the epidermal cornified envelope. Gene targeting in mouse embryonic stem cells was used to generate a null allele of envoplakin. No envoplakin transcripts from the targeted allele could be detected in the skin of newborn mice. Mice homozygous for the targeted allele were born in the normal Mendelian ratio and were fertile. They did not develop any discernible pathological phenotype up to the age of 1 year. The ultrastructural appearance of cornified envelopes from adult epidermis was indistinguishable between wild-type and knockout mice, and there was no evidence that the absence of envoplakin affected the subcellular distribution of periplakin or desmoplakin, two other plakins found in desmosomes. The proportion of immature cornified envelopes in the epidermis of newborn mice was greater in envoplakin-null animals than in heterozygous littermates or wild-type mice, and the envelopes had a larger surface area. This correlated with a slight delay in barrier acquisition during embryonic development. We conclude that although envoplakin is part of the scaffolding on which the cornified envelope is assembled, it is not essential for envelope formation or epidermal barrier function.

The functional endpoint of epidermal differentiation is assembly of the cornified envelope (CE), a covalently cross-linked protein layer that is deposited at the cytoplasmic face of the plasma membrane and forms a barrier between the living cell layers of the skin and the outside environment (16, 26, 27, 35). The importance of the epidermal barrier is highlighted by the phenotype of mice which lack the gene for transglutaminase 1 (25), the key enzyme responsible for the cross-linking of envelope precursor proteins, in which a failure in cornified envelope assembly leads to excessive transepidermal water loss and neonatal lethality. Inactivating mutations in the human gene also result in severe perturbation of epidermal differentiation and function (15). Although there are a multitude of proteins that become incorporated into the cornified envelope, recent biochemical, cell biological, and immunoelectron microscopical data suggest that cornified envelope biogenesis is an ordered process, in which cross-linking of one specific group of proteins at the membrane precedes incorporation of abundant late precursors such as loricrin and the small proline-rich proteins (4, 24, 32, 33, 34).

Two of the early envelope precursors are envoplakin and periplakin (1, 28, 29). They belong to the plakin family of cytolinker proteins, which includes desmoplakin, plectin, and BPAG1 (6, 12, 14, 20, 30, 37). Prior to cornified envelope assembly, envoplakin and periplakin localize to desmosomes and form an interconnecting subplasmalemmal network between the desmosomes (28, 29, 31). Envoplakin and periplakin can heterodimerize via their rod domains, and the periplakin N-terminal globular domain appears to target heterodimers to desmosomes and the interdesmosomal plasma membrane (4). This distribution suggests a model in which the role of the proteins is to form the initial scaffold on which the cornified envelope is built (29). The model is supported by biochemical evidence showing cross-links between envoplakin, periplakin, and another early CE precursor, involucrin, in peptides released by sequential proteolysis of purified envelopes, and by immunoelectron microscopy demonstrating the presence of the proteins at the inner surface of maturing envelopes (24, 32, 33, 34).

To examine whether envoplakin is essential for cornified envelope assembly, we generated mice with a targeted deletion of the envoplakin gene. Surprisingly, cornified envelope assembly was not inhibited, and the mice had no pathological phenotype.

MATERIALS AND METHODS

Construction of a targeting vector for the Evpl locus. The cloning and characterization of the mouse envoplakin gene from a 129/Sv lambda library has been described previously (21). To construct the targeting vector, a 3.2-kb *Hin*dIII-*Sty*I (blunt ended) restriction fragment extending from the 5′-flanking region to the first exon of the gene was ligated to *Hin*dIII- and *Sma*I-cut pBluescript II (Stratagene) vector. Next, a 6-kb *Avr*II fragment covering exons 9 to 18 of the gene was ligated to the *Xba*I site of the plasmid to constitute the 3′ arm of the targeting vector. Finally, a 5-kb cassette containing stop codons in all reading frames followed by an internal ribosome entry site-driven *lacZ* coding sequence and a neomycin resistance gene under an MC1 promoter was introduced into the *Bam*HI site between the envoplakin gene fragments (Fig. 1a). Prior to electroporation, the targeting vector was linearized by *Sal*I digestion.

Generation of gene-targeted mice. Embryonic stem (ES) cells were cultured on STO fibroblast feeder cells in the presence of leukemia inhibitor factor (ESGRO; Gibco-BRL) and electroporated as described previously (3). Selected clones were expanded in 96-well plates and screened by Southern blotting of *Bam*HI-digested genomic DNA using a 0.5-kb *Bam*HI-*Hin*dIII genomic fragment immediately 5′ to the 5′ arm of the targeting vector (Fig. 1a and b). The correct integration of the 3′-end arm was confirmed by Southern blotting of *Eco*RI-digested DNA using an *Xho*I-*Spe*I fragment from the 18th intron of the gene (Fig. 1a and b).

* Corresponding author. Mailing address: Imperial Cancer Research Fund, 44 Lincoln's Inn Fields, London WC2A 3PX, United Kingdom. Phone: 44 20 7269 3528. Fax: 44 20 7269 3078. E-mail: watt@icrf.icnet.uk.

† Present address: Department of Biological Sciences, University of Durham, Durham DH1 3LE, United Kingdom.

‡ Present address: New Link Genetics, Ames, IA 50014.

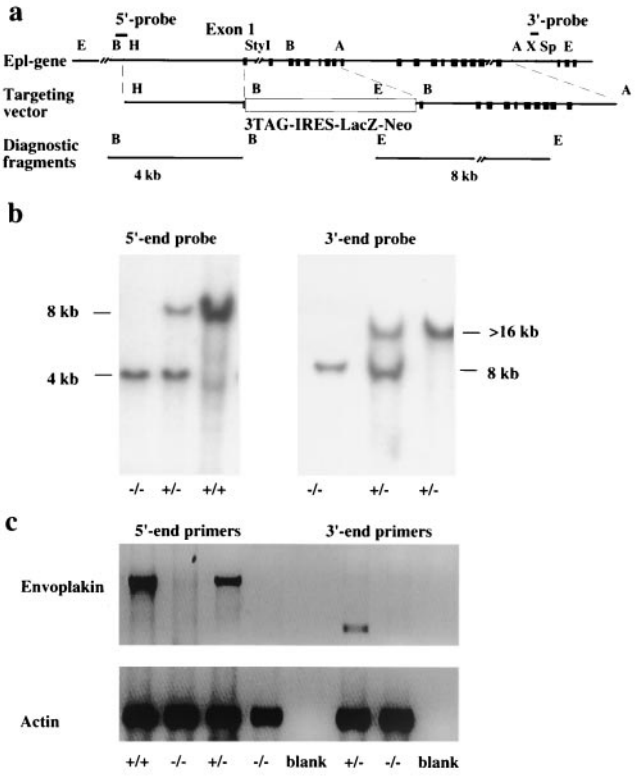

FIG. 1. Gene targeting of envoplakin locus. (a) Targeting strategy used to generate the envoplakin null allele. Top, 5′ end of the envoplakin gene. Black boxes represent the exons. Middle, the targeting vector inserts into the first exon of the envoplakin gene a cassette with stop codons in all reading frames, an internal ribosome entry site-dependent *lacZ* reporter gene, and a neomycin resistance gene. Bottom, diagnostic 5′ and 3′ end fragments to recognize correctly integrated targeting vector. (b) Genotyping the offspring of heterozygous crosses by Southern blotting. The −/− animals are homozygous for the targeted allele, as revealed by both the 5′ and 3′ probes. (c) RT-PCR analysis of mRNA from the skin of newborn mice. Both 5′-end primers (five first lanes from the left) that flank the deleted part of the gene and 3′-end primers (three right-hand lanes) from the last exon of the gene were used to verify the absence of mRNA in null animals. Primers for γ-actin were used as a control for the quality of the template RNA. Genotypes were determined by Southern blotting using the 5′-end probe.

RT-PCR analysis of envoplakin mRNA. Total RNA was isolated from newborn mouse skin and bladder using RNAZol B reagent (BioGenesis). For reverse transcription (RT)-PCR, first-strand cDNA was synthesized by SuperScript II (Gibco-BRL) reverse transcriptase using random hexamer primers or oligo (dT) primer. Two different primer pairs were used to amplify mouse envoplakin as follows: for the 5′ end of the cDNA primers, 5′-ACCATGTTCAAGGGGC TGAGCAA (from the first exon) and 5′-TCAGGGTCTGGTGCTGGGAT (from the 12th exon); for the 3′-end primers, 5′-GCTGGTACAGCACCTGAC TGGG and 5′-GATTGCGCAGTGAGGTGGACAC (both from the last exon of the gene). Mouse γ-actin cDNA was amplified using primers 5′-GTTTGAG ACCTTCAACACCCC and 5′-GTGGCCATCTCCTGCTCGAAGTC.

Animal protocols. All the protocols used in this study were approved by the local animal ethics and genetic modification committees at the Imperial Cancer Research Fund and covered by a Home Office project license. Wound healing was monitored in 7- to 8-week-old female mice in which two full thickness wounds were excised in the dorsal skin under general anesthesia (Halothane-Vet; Merial), using a 3-mm biopsy punch (Stiefel). Mice were sacrificed 4, 7, and 14 days after wounding. A total of eight wounds per time point per genotype were examined.

Histology. Mouse tissues were fixed in formalin and embedded in paraffin. For frozen sections, the tissue samples were placed in OCT compound in a liquid nitrogen-cooled isopentane bath. For routine histology, 4-μm sections were stained with hematoxylin and eosin. β-Galactosidase activity was visualized as described previously (21).

Isolation and culture of primary newborn mouse keratinocytes. Mouse keratinocytes were isolated from 2- to 4-day-old animals as described (11) and cultured on collagen-coated dishes (Becton Dickinson) in low-calcium (0.05 mM $CaCl_2$) F-12–adenine–Dulbecco's (FAD) medium supplemented with 10% Chelex-treated fetal bovine serum plus 0.5 μg of hydrocortisone, 5 μg of insulin, and 10 ng of epidermal growth factor per ml and 10^{-10} M cholera toxin (13). To induce differentiating cells to stratify, the cultures were switched to normal (high calcium) FAD medium 16 h before harvesting (13).

Indirect immunofluorescence staining of cultured keratinocytes. For the detection of plakin epitopes, cells grown on collagen-coated glass coverslips were extracted with CSK buffer (50 mM NaCl, 300 mM sucrose, 10 mM PIPES [piperazine-*N*, *N*′-bis(2-ethanesulfonic acid), pH 6.8], 3 mM $MgCl_2$, 0.5% Triton X-100, 10 mM EDTA) for 5 min and fixed for 5 min with ice-cold methanol. Alternatively, the cells were fixed at room temperature with 3% paraformaldehyde for 20 min, followed by extraction with 0.2% Triton X-100 in phosphate-buffered saline (PBS) for 5 min at room temperature, and 0.5% fish skin gelatin (Sigma) was used to block nonspecific binding.

The following primary antibodies were used: TD2, a rabbit polyclonal antibody that recognizes mouse and human periplakin; DP121, a rabbit polyclonal antibody against desmoplakin (kind gift of Tony Magee, NIMR, London); and C-20, a goat polyclonal antibody against plectin (Santa Cruz). TD2 was raised against a 48-amino-acid peptide corresponding to amino acids 1646 to 1694 of human periplakin (see numbering system of DiColandrea et al. [4]) that had been conjugated to keyhole limpet hemocyanin prior to injection. Alexa 488- or Alexa 594-conjugated goat anti-rabbit, goat anti-mouse, or donkey anti-goat immunoglobulin G (IgG) (Molecular Probes) was used as the secondary antibody. Coverslips were mounted in Gelvatol (Monsanto) and examined using a laser scanning confocal microscope (LSM 510; Carl Zeiss). Digital images were captured by an LSM software package using equal settings for control and envoplakin-null cells. The images were prepared for publication using Adobe Photoshop 5.02 without changing the contrast, lightness, or resolution of the original images.

Isolation of cornified envelopes. Pieces of newborn mouse dorsal skin or adult mouse ear tips (5 by 5 mm) were boiled for 20 min in CE isolation buffer containing 20 mM Tris-HCl (pH 7.5), 5 mM EDTA, 10 mM dithiothreitol (DTT), and 2% sodium dodecyl sulfate (SDS) (19). Cornified envelopes were pelleted by a 5-min centrifugation at 5,000 × *g*, washed in CE isolation buffer with 0.2% SDS, repelleted, resuspended in the washing buffer, and stored at 4°C. To isolate cornified envelopes from primary mouse keratinocytes, confluent cultures on 100-mm collagen-coated culture dishes (Becton Dickinson) were switched to high-calcium growth conditions for 24 h or 5 days. Adherent and floating cells were pooled, and cornified envelopes were isolated by boiling in SDS and DTT as described above.

The type (fragile or mature) and surface area of individual cornified envelopes were determined by phase contrast microscopy. CE from a total of six 3-day-old animals per genotype were scored by counting all the envelopes per field in 10 randomly selected photographic fields, corresponding to 466 wild-type and 388 knockout envelopes. Surface areas were measured in pixels using National Institutes of Health imaging software.

Dye exclusion assay for development of epidermal barrier. Mouse embryos were dehydrated by 1-min incubations in an ascending series of methanol, rehydrated with the same series of methanol, washed in PBS, and stained with 0.0125% toluidine blue as described (10, 19).

Electron microscopy. CE were isolated as described above and then sonicated three times for 10 each. Envelope suspensions were washed in PBS and then infiltrated with 2% gelatin and allowed to set at 4°C. The specimens were infused with 2.3 M sucrose for 4 h, frozen in liquid nitrogen, and sectioned as described previously (28, 29). Sections were stained with saturated aqueous uranyl acetate and examined with a Jeol 120 electron microscope.

RESULTS

Gene targeting of envoplakin locus. To generate envoplakin knockout mice, we constructed a targeting vector designed to introduce into the first exon of the gene a stop codon followed by an internal ribosome entry site and a *lacZ* reporter gene and to delete the following eight exons of the gene (Fig. 1a). The targeting vector was electroporated into 129/Sv mouse embryonic stem cells, and G418-resistant clones harboring the cor-

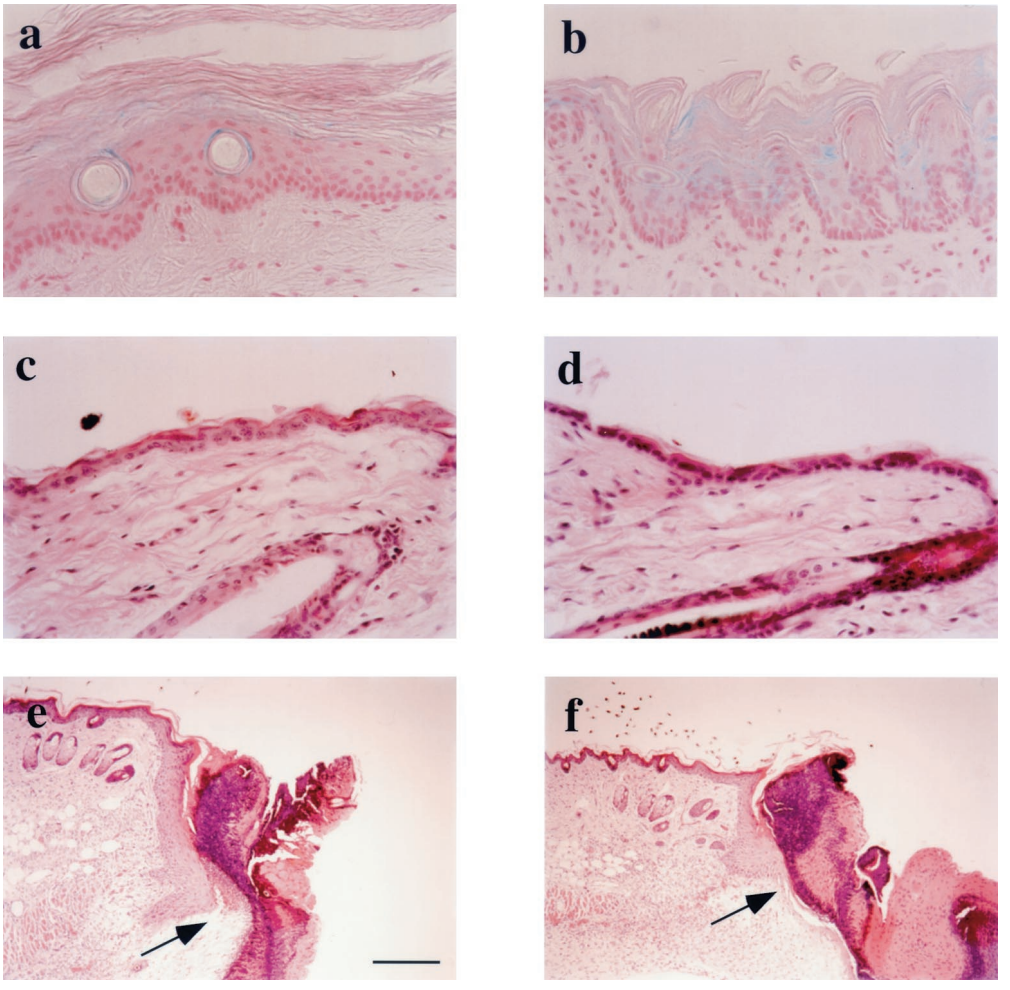

FIG. 2. Epithelial histology of envoplakin null mice. (a and b) Whole-mount β-galactosidase staining was used to detect expression of the knockin *lacZ* reporter gene in tail (a) and tongue (b) epithelium of homozygous gene-targeted animals. (c to f) Hematoxylin and eosin staining of sections of intact (c and d) and wounded (e and f) back skin of heterozygous (c and e) and homozygous (d and f) mice. Arrows in e and f indicate the migrating front of wound edge keratinocytes 4 days after wounding. Bar, 60 μm (a to d) or 250 μm (e and f).

rectly integrated vector were screened by Southern blotting using external 5′ and 3′ probes (Fig. 1a and b). Nine of 184 clones were correctly targeted, and all but one had maintained a normal karyotype (data not shown). Two independent clones were injected into blastocysts, and both resulted in germ line transmission of the targeted allele. Crossing of heterozygous animals produced all genotypes (+/+, +/−, and −/−) in the expected Mendelian ratio (data not shown).

RT-PCR was used to amplify envoplakin mRNA from wild-type mice and their littermates that were homozygous or heterozygous for the targeted allele. No envoplakin mRNA was detected in skin (Fig. 1c) or bladder (not shown) of the −/− animals. Owing to the large size and multiexon structure of the envoplakin gene (21), primer pairs from both the 5′ end and the 3′ end of the mRNA were used to confirm that the gene targeting had resulted in an envoplakin-null allele (Fig. 1c).

The knockin *lacZ* gene translated from an internal ribosome entry site produced active β-galactosidase enzyme and was used to report activity of the endogenous envoplakin promoter. In stratified epithelia, β-galactosidase activity was restricted to differentiated and cornifying cell layers, as illustrated for tail skin (Fig. 2a) and tongue (Fig. 2b).

Envoplakin knockout mice have no obvious pathological phenotype. The homozygous animals were indistinguishable from their wild-type or heterozygous littermates and did not acquire any pathological skin or coat phenotype up to 1 year of age. Males and females were fertile, with females having normal litter sizes and showing no defects in lactation.

Hematoxylin-and-eosin-stained tissue sections of adult and newborn back skin had unaltered histology compared to wild-type littermates (Fig. 2c and d and data not shown). No changes were seen in the number or distribution of actively cycling keratinocytes in interfollicular epidermis or in the hair follicles as determined by Ki67 antigen immunohistochemistry (data not shown). No histological changes were seen in the thick, non-hair-bearing epidermis of the soles of the feet (data not shown) or in any of the other epithelia in which envoplakin is known to be expressed (28, 29), including tongue, oral mucosa, mammary gland, esophagus, and bladder (Fig. 2a and b and data not shown).

Wound healing was investigated by monitoring the closure of full-thickness punch biopsies of dorsal skin in which the hair follicles were in telogen (resting phase of the hair growth cycle). The biopsy wounds healed at an equal rate in wild-type and knockout females; at day 4, a prominent migrating epidermal sheet was detectable under the wound clot (Fig. 2e and f), and by day 7 the wound was fully closed regardless of genotype (data not shown).

Lack of envoplakin causes subtle changes in cornified envelopes. Cornified envelopes were isolated from newborn skin and analyzed by transmission electron microscopy (Fig. 3a and b). Wild-type and envoplakin-null cornified envelopes had the same thickness and were ultrastructurally indistinguishable. Residual desmosomes were observed in both types of CE preparation and had normal morphology (arrows in Fig. 3a and b).

When CE are observed under a light microscope, two types can be distinguished, fragile and rigid (19, 34). The fragile envelopes have a more wrinkled appearance and are less refractile than the mature, rigid envelopes. Fragile envelopes are immature precursors of rigid envelopes. There was a small but statistically significant (18 versus 12%, χ^2 test) increase in the proportion of fragile envelopes in newborn knockout compared to wild-type skin (Fig. 3c). The average area of the rigid envelopes was 24% larger in skin from knockout compared to wild-type animals, and the difference was statistically significant ($P < 0.001$, t test).

We also monitored cornified envelope formation by cultures of primary keratinocytes from wild-type and envoplakin knockout mice. The proportions of cells that formed CE in high-calcium medium were the same. After 5 days in high-calcium medium, 16% of knockout and 20% of wild-type envelopes were mature. Many envelopes retained a whole or fragmented nucleus (data not shown).

The higher proportion of fragile envelopes in envoplakin-null epidermis suggested that there might be a delay in epidermal barrier formation. This was analyzed by using a whole-mount dye exclusion assay (10). Both knockout and heterozygous animals had acquired an intact epidermal barrier by embryonic day 17.5 (E17.5), when toluidine blue dye was unable to penetrate the developing skin. However, at E16.5, the barrier was less highly developed in envoplakin-null animals. As illustrated in Fig. 3d, the skin covering the back of the head and most of the dorsum of wild-type embryos was impenetrable to toluidine blue at E16.5. In contrast, envoplakin-null embryos at E16.5 were completely blue or had only a small white area at the back of the head.

Subcellular distribution of other plakin family members is unaffected by loss of envoplakin. To evaluate whether the expression of other plakin proteins was altered in keratinocytes lacking envoplakin, we examined periplakin and desmoplakin in null mice and their heterozygous littermates by immunofluorescence staining of frozen skin sections and fixed cultures of primary keratinocytes.

Periplakin was detected in mouse tissues using TD2, a rabbit antiserum to a peptide in the periplakin linker domain that is conserved between mice and humans (21). This antibody recognizes the predicted 195-kDa polypeptide in immunoblots of mouse skin extracts (not shown). The distribution of periplakin was the same in wild-type epidermis and epidermis of envoplakin knockout and heterozygous mice: the protein was up-regulated during terminal differentiation and expressed at high levels at the cell membrane of cells in the suprabasal layers (29) (data not shown). Desmoplakin was expressed at the plasma membrane of keratinocytes in all epidermal layers and was indistinguishable between wild-type, envoplakin −/−, and envoplakin +/− epidermis (29) (data not shown).

In stratified cultures of keratinocytes, desmoplakin was localized at cell-cell borders, in the characteristic punctate pattern indicative of desmosome formation (29). There was no difference in the distribution of desmoplakin in keratinocytes cultured from wild-type and envoplakin-null epidermis (Fig. 4a and b). Periplakin immunoreactivity was restricted to suprabasal, terminally differentiating keratinocytes and, although somewhat punctate, was more diffuse than desmoplakin, as reported previously (29). There was no difference in the distribution of periplakin in wild-type and envoplakin-deficient keratinocytes (Fig. 4c and d).

DISCUSSION

We have targeted the mouse envoplakin locus (21) with a vector that introduces a stop codon in the first exon of the gene and deletes the following eight exons, replacing them with the β-galactosidase gene. The pattern of β-galactosidase expression was consistent with the known distribution of envoplakin protein (28, 29) and the sites of activity of the envoplakin promoter (21).

Envoplakin knockout mice did not have any obvious pathological phenotype in the skin or other epithelia in which envoplakin is normally expressed. In particular, the mice did not show any signs of epidermal fragility or blistering. Such characteristics had been anticipated because of the known association of envoplakin with the desmosomal plaque (4, 28, 29) and the pathology of a human skin-blistering disease, paraneoplastic pemphigus, in which autoantibodies to envoplakin and other desmosomal proteins destabilize cellular junctions (18, 23).

Envoplakin is the first member of the plakin family that has been found to be dispensable for normal viability. Mice without desmoplakin die at day E6.5 of embryonic development (7); embryo rescue in aggregation chimeras demonstrates an essential role for desmoplakin in embryonic heart, neuroepithelium, skin, and vasculature (8). Lack of either plectin or BPAG1 results in epidermal blistering owing to dissociation of keratin bundles from hemidesmosomes (2, 9); in addition, the BPAG1-null animals have severe neuronal degeneration, and plectin-deficient mice demonstrate muscular dystrophy.

We and others have recently put forward a hypothesis that predicts a central role for envoplakin in the formation of the scaffold on which the cornified envelope is assembled (4, 24, 29). Envoplakin and periplakin are membrane-associated CE precursors that surround the core desmosomes and can thus form large initial cross-linked plaques. Furthermore, as involucrin, an abundant early CE precursor, is frequently cross-linked to envoplakin (33, 34), it could be predicted that loss of envoplakin would severely compromise the early steps of envelope biogenesis. However, the observed phenotype was rather mild. There was only a slight delay in CE maturation, as evaluated by the ratio of fragile to mature envelopes and dye exclusion by embryonic epidermis. These results strongly sug-

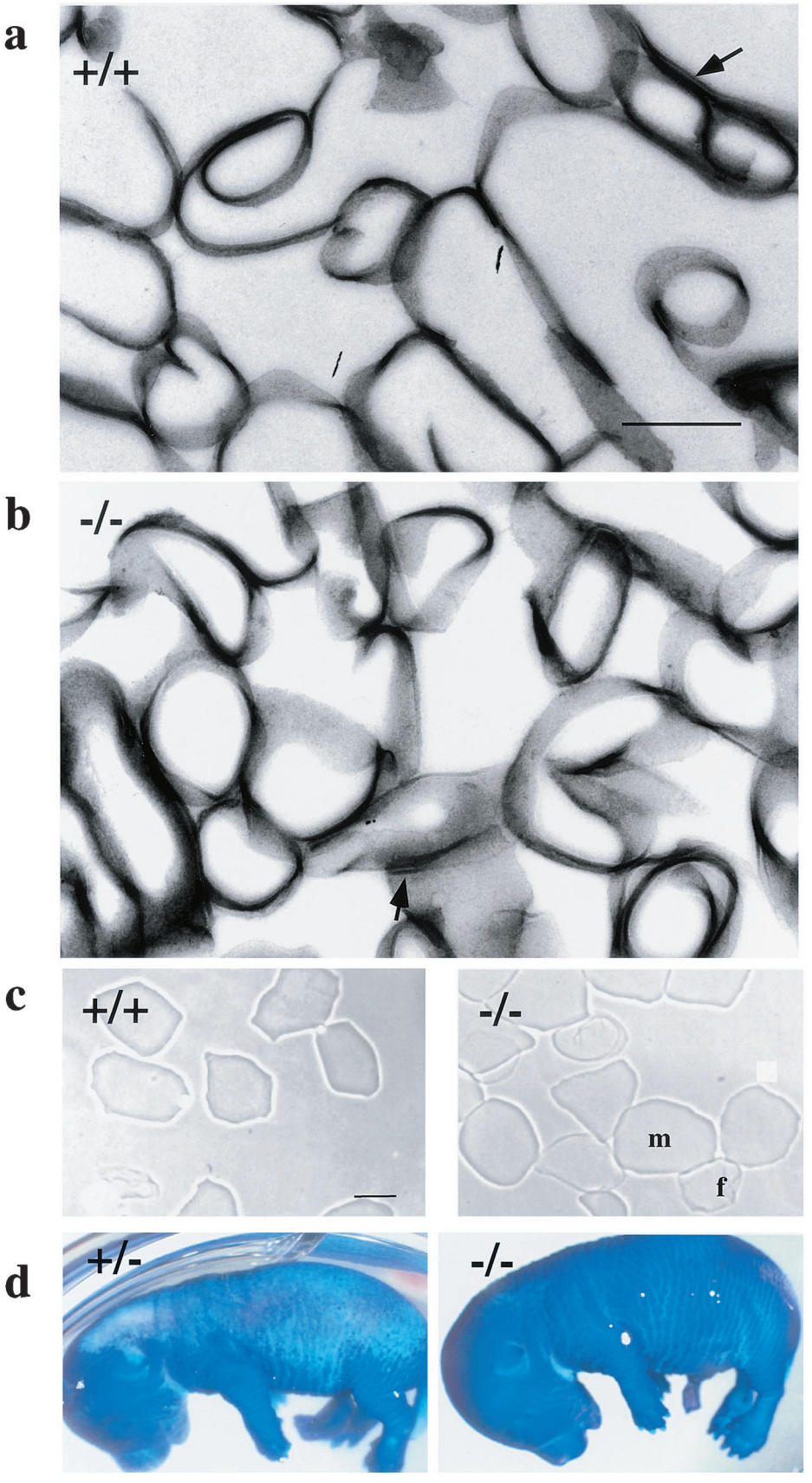

FIG. 3. Barrier acquisition and cornified envelope morphology. (a and b) Transmission electron microscopy of isolated CE from +/+ (a) and −/− (b) epidermis. Arrows indicate residual desmosomes. (c) Cornified envelopes isolated from 2-day-old wild-type or envoplakin knockout mice. f, fragile envelope; m, mature envelope. (d) E16.5 heterozygous (+/−) and envoplakin null homozygous (−/−) embryos stained with toluidine blue. Dark blue areas of the skin have not yet formed the epidermal barrier. Bar, 500 nm (a and b) or 25 μm (c).

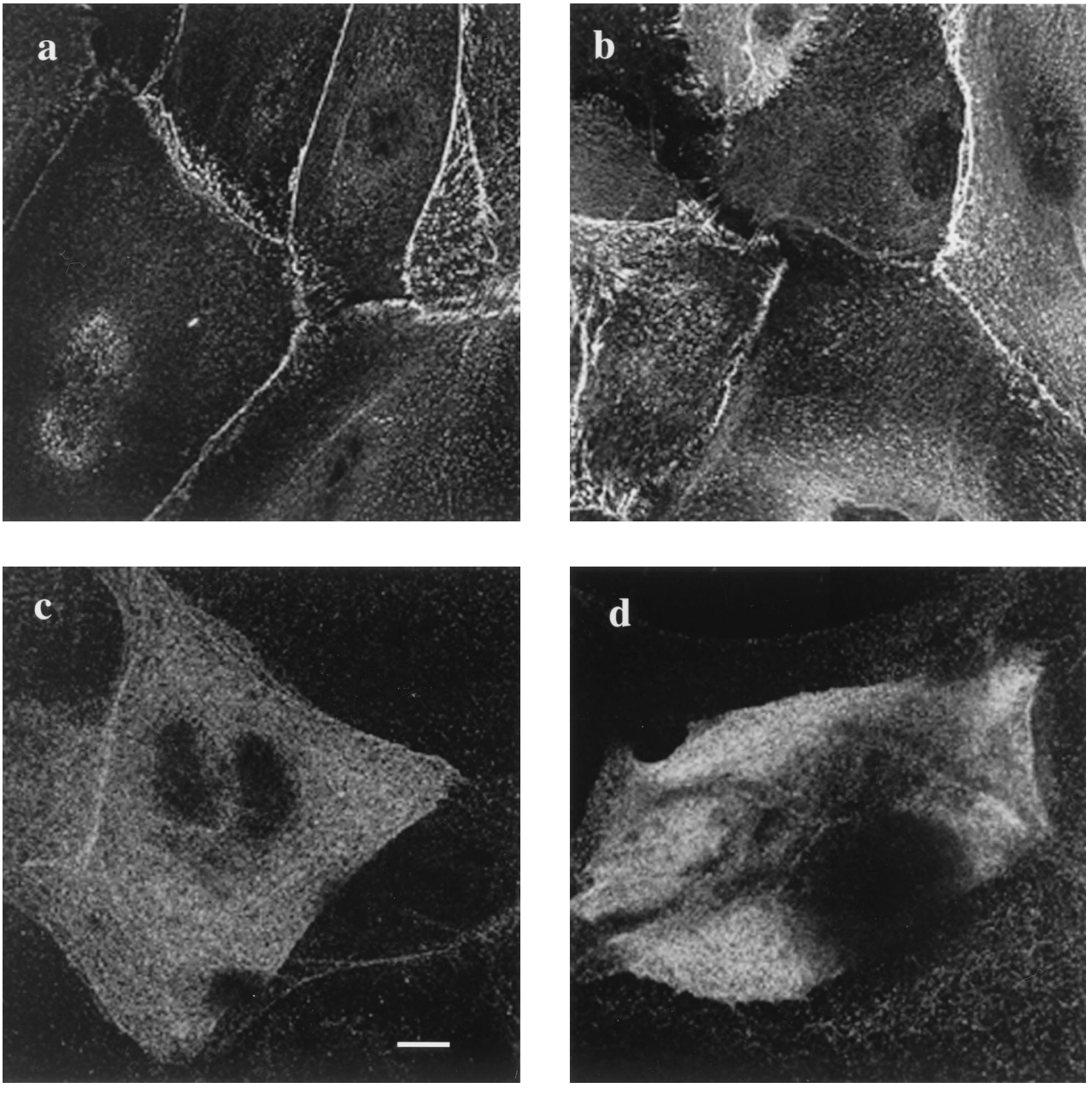

FIG. 4. Subcellular distribution of desmoplakin and periplakin in cultured keratinocytes. Primary keratinocytes grown in high-calcium medium were stained with antibodies against desmoplakin (a and b) and periplakin (c and d). (a and c) Wild-type keratinocytes; (b and d) envoplakin-deficient keratinocytes. Bar, 10 μm (a to c) or 7 μm (d).

gest that envoplakin can be replaced by other CE precursor proteins to assemble a cornified envelope that confers skin barrier function. Periplakin is the most likely protein to compensate for loss of envoplakin, since periplakin heterodimerizes with envoplakin, targeting envoplakin to the plasma membrane (4) and modulating its association with intermediate filaments (T. Karashima and F. M. Watt, submitted for publication).

Envoplakin is not the only CE component to be dispensable for normal epidermal barrier formation. No abnormalities in the histology of the epidermis or the morphology of the envelopes are detectable in mice lacking involucrin (5). Lack of loricrin, the most abundant precursor of mature envelopes, results only in temporary erythroderma of neonatal mice, slightly delayed barrier development, and increased fragility of isolated envelopes (19). Lack of loricrin appears to be compensated for by increased expression of another group of CE precursors, the small proline-rich proteins (19). Mutation of loricrin is more deleterious than loss of the protein: in humans with Vohlwinkel's syndrome (22) or progressive symmetric erythrokeratoderma (16) and in mouse models of these diseases (36), mutant loricrin accumulates in the nucleus of keratinocytes, and it is this, rather than abnormal CE assembly, that appears to be responsible for the epidermal pathology

(36). Thus, current evidence suggests that no single CE precursor protein is absolutely necessary for envelope biogenesis, and only lack of the enzyme that cross-links the precursors, transglutaminase 1, completely disrupts barrier formation (25). Since it is possible that envoplakin and periplakin homodimers can each perform the functions of the other and substitute for envoplakin/periplakin heterodimers, it will be important to investigate whether mice that lack both proteins have any impairment of CE assembly.

ACKNOWLEDGMENTS

We are grateful to Ian Rosewell for blastocyst injections, Mike Owen for embryonic stem cells, Eddie Wang for practical advice on ES cell cultures, Jill Williamson for karyotyping the ES cell clones, and George Elia and the members of the ICRF Histopathology Laboratory for their help in preparing and sectioning paraffin blocks. We thank the personnel of the Biological Resources Unit for their expert technical assistance.

The research was funded by the Imperial Cancer Research Fund, and by an EU Network grant to F.M.W. by an EMBO Long-Term Fellowship to A.M.

REFERENCES

1. **Aho, S., W. H. McLean, K. Li, and J. Uitto.** 1998. cDNA cloning, mRNA expression and chromosomal mapping of human and mouse periplakin genes. Genomics **48:**242–247.
2. **Andrä, K., H. Lassmann, R. Bittner, S. Shorny, R. Fässler, F. Propst, and G. Wiche.** 1997. Targeted inactivation of plectin reveals essential function in maintaining the integrity of skin, muscle and heart cytoarchitecture. Genes Dev. **11:**3143–3156.
3. **Denzel, A., F. Otto, A. Girod, R. Pepperkok, R. Watson, I. Rosewell, J. J. M. Bergeron, R. C. E. Solari, and M. J. Owen.** 1999. The p24 family member p23 is required for early embryonic development. Curr. Biol. **10:**55–58.
4. **DiColandrea, T., T. Karashima, A. Määttä, and F. M. Watt.** 2000. Subcellular distribution of envoplakin and periplakin: insights into their role as precursors of the epidermal cornified envelope. J. Cell Biol. **151:**573–585.
5. **Djian P., K. Easley, and H. Green.** 2000. Targeted ablation of the murine involucrin gene. J. Cell Biol. **151:**381–387.
6. **Fuchs, E., and Y. Yang.** 1999. Crossroads on cytoskeletal highways. Cell **98:**547–550.
7. **Gallicano, G. I., P. Kouklis, C. Bauer, M. Yin, V. Vasioukin, L. Degenstein, and E. Fuchs.** 1999. Desmoplakin is required early in development for assembly of desmosomes and cytoskeletal linkage. J. Cell Biol. **143:**2009–2022.
8. **Gallicano, G. I., C. Bauer, and E. Fuchs.** 2001. Rescuing desmoplakin function in extra-embryonic ectoderm reveals the importance of this protein in embryonic heart, neuroepithelium, skin and vasculature. Development **128:** 929–941.
9. **Guo, L., L. Degenstein, J. Dowling, Q.-C. Yu, R. Wollman, B. Perman, and E. Fuchs.** 1995. Gene targeting of BPAG1: abnormalities in mechanical strength and cell migration in stratified squamous epithelia and severe neurologic degeneration. Cell **81:**233–243.
10. **Hardman, M. J., P. Sisi, D. N. Banbury, and C. Byrne.** 1998. Patterned acquisition of skin barrier function during development. Development **125:** 1541–1552.
11. **Hennings, H., D. Michael, C. Cheng, P. M. Steinert, K. Holbrook, and S. H. Yuspa.** 1980. Calcium regulation of growth and differentiation of mouse epidermal cells in culture. Cell **19:**245–254.
12. **Herrmann, H., and U. Aebi.** 2000. Intermediate filaments and their associates: multi-talented structural elements specifying cytoarchitecture and cytodynamics. Curr. Opin. Cell Biol. **12:**79–90.
13. **Hodivala, K. J., and F. M. Watt.** 1994. Evidence that cadherins play a role in the downregulation of integrin expression that occurs during keratinocyte terminal differentiation. J. Cell Biol. **124:**589–600.
14. **Houseweart, M. K., and D. W. Cleveland.** 1998. Intermediate filaments and their associated proteins: multiple dynamic personalities. Curr. Opin. Cell Biol. **10:**93–101.
15. **Huber, M., I. Rettler, K. Bernasconi, E. Frenk, S. P. Lavrijsen, M. Ponec, A. Bon, S. Lautenschlager, D. F. Schorderet, and D. Hohl.** 1995. Mutations of keratinocyte transglutaminase in lamellar ichthyosis. Science **267:**525–528.
16. **Ishida-Yamamoto, A., J. A. McGrath, H. Lam, H. Iizuka, R. A. Friedman, and A. M. Christiano.** 1997. The molecular pathology of progressive symmetric erythrokeratoderma: a frameshift mutation in the loricrin gene and perturbations in the cornified cell envelope. Am. J. Hum. Genet. **61:**581–589.
17. **Ishida-Yamamoto, A., and H. Iizuka.** 1998. Structural organization of cornified cell envelopes and alterations in inherited skin disorders. Exp. Dermatol. **7:**1–10.
18. **Kiyokawa, C., C. Ruhrberg, Z. Nie, T. Karashima, O. Mori, T. Nishikawa, K. J. Green, G. J. Anhalt, T. DiColandrea, F. M. Watt, and T. Hashimoto.** 1998. Envoplakin and periplakin are components of the paraneoplastic pemphigus antigen complex. J. Investig. Dermatol. **111:**1236–1238.
19. **Koch, P. J., P. A. de Viragh, E. Scharer, D. Bundman, M. A. Longley, J. Bickenbach, Y. Kawachi, Y. Suga, Z. Zhou, M. Huber, D. Hohl, T. Kartasova, M. Jarnik, A. C. Steven, and D. R. Roop.** 2000. Lessons from loricrin-deficient mice: compensatory mechanisms maintaining skin barrier function in the absence of a major cornified envelope protein. J. Cell Biol. **151:**389–400.
20. **Kowalczyk, A. P., E. A. Bornslaeger, S. M. Norvell, H. L. Palka, and K. J. Green.** 1999. Desmosomes: intercellular adhesive junctions specialized for attachment of intermediate filaments. Int. Rev. Cytol. **185:**237–302.
21. **Määttä, A., C. Ruhrberg, and F. M. Watt.** 2000. Structure and regulation of the envoplakin gene. J. Biol. Chem. **275:**19857–19865.
22. **Maestrini, E., A. P. Monaco, J. A. McGrath, A. Ishida-Yamamoto, C. Camisa, A. Hovnanian, D. E. Weeks, M. Lathrop, J. Uitto, and A. M. Christiano.** 1996. A molecular defect in loricrin, the major component of the cornified cell envelope, underlies Vohlwinkel's syndrome. Nat. Genet. **13:** 70–77.
23. **Mahoney, M. G., S. Aho, J. Uitto and J. R. Stanley.** 1998. The members of the plakin family of proteins recognized by paraneoplastic pemphigus antibodies include periplakin. J. Investig. Dermatol. **111:**308–313.
24. **Marekov, L. N., and P. M. Steinert.** 1998. Ceramides are bound to structural proteins of human foreskin epidermal cornified envelopes. J. Biol. Chem. **273:**17763–17770.
25. **Matsuki, M., F. Yamashita, A. Ishida-Yamamoto, K. Yamada, C. Kinoshita, S. Fushiki, E. Ueda, Y. Morishima, K. Tabata, H. Yasuno, M. Hashida, H. Iizuka, M. Ikawa, M. Okabe, G. Kondoh, T. Kinoshita, and K. Yamanishi.** 1998. Defective stratum corneum and early neonatal death in mice lacking the gene for transglutaminase 1 (keratinocyte transglutaminase). Proc. Natl. Acad. Sci. USA **95:**1044–1049.
26. **Nemes, Z., and P. M. Steinert.** 1999. Bricks and mortar of the epidermal barrier. Exp. Mol. Med. **31:**5–19.
27. **Rice, R. H., and H. Green.** 1977. The cornified envelope of terminally differentiated human epidermal keratinocytes consists of cross-linked proteins. Cell **11:**417–422.
28. **Ruhrberg, C., M. A. N. Hajibagheri, M. Simon, T. P. Dooley, and F. M. Watt.** 1996. Envoplakin, a novel precursor of cornified envelopes that has homology to desmoplakin. J. Cell Biol. **134:**715–729.
29. **Ruhrberg, C., M. A. N. Hajibagheri, D. A. D. Parry, and F. M. Watt.** 1997. Periplakin, a novel component of cornified envelopes and desmosomes that belongs to the plakin family and forms complexes with envoplakin. J. Cell Biol. **139:**1835–1849.
30. **Ruhrberg, C., and F. M. Watt.** 1997. The plakin family: versatile organizers of cytoskeletal architecture. Curr. Opin. Genet. Dev. **7:**392–397.
31. **Simon, M., and H. Green.** 1984. Participation of membrane-associated proteins in the formation of the cross-linked envelope of the keratinocyte. Cell **36:**827–834.
32. **Steinert, P. M., and L. N. Marekov.** 1995. The proteins elafin, filaggrin, keratin intermediate filaments, loricrin and SPRs are isopeptide cross-linked components of human cornified cell envelope. J. Biol. Chem. **270:**17702–17711.
33. **Steinert, P. M., and L. N. Marekov.** 1997. Involucrin is an early component in the assembly of the epidermal cornified cell envelope. J. Biol. Chem. **272:**2021–2030.
34. **Steinert, P. M., and L. N. Marekov.** 1999. Initiation and assembly of the cell envelope barrier structure of stratified squamous epithelia. Mol. Biol. Cell **10:**4247–4261.
35. **Steinert, P. M.** 2000. The complexity and redundancy of epithelial barrier function. J. Cell Biol. **151:**F5–F7.
36. **Suga, Y., M. Jarnik, P. S. Attar, M. A. Longley, D. Bundman, A. C. Steven, P. J. Koch, and D. R. Roop.** 2000. Transgenic mice expressing a mutant form of loricrin reveal the molecular basis of the skin diseases, Vohlwinkel syndrome and progressive symmetric erythrokeratoderma. J. Cell Biol. **151:**410–412.
37. **Wiche, G.** 1998. Role of plectin in cytoskeletal organization and dynamics. J. Cell Sci. **111:**2477–2486.